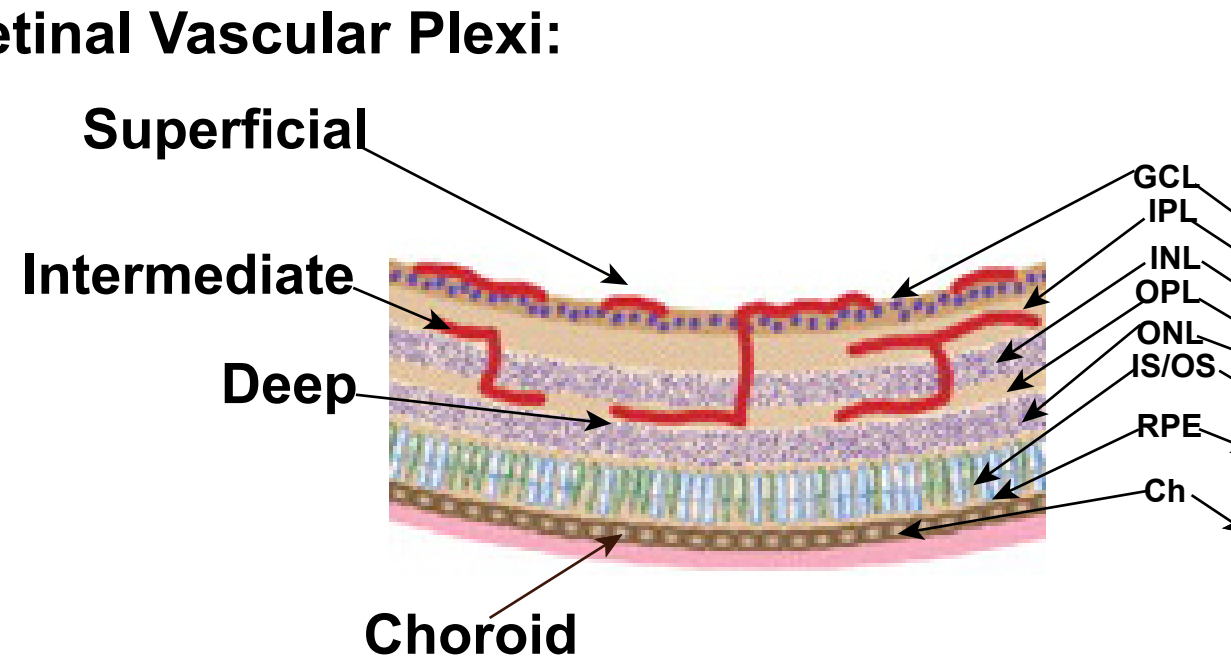
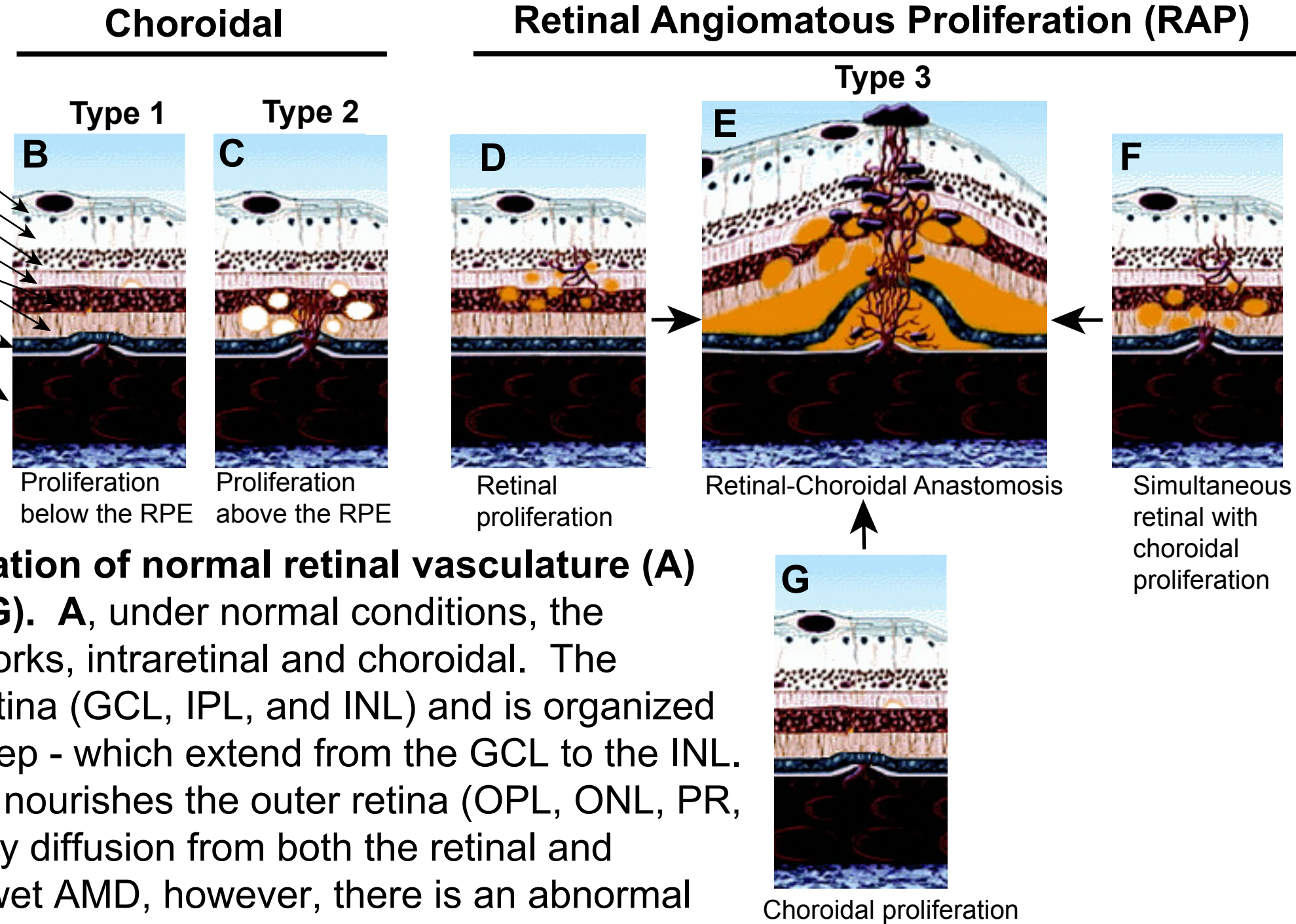


A Normal Retinal Vasculature

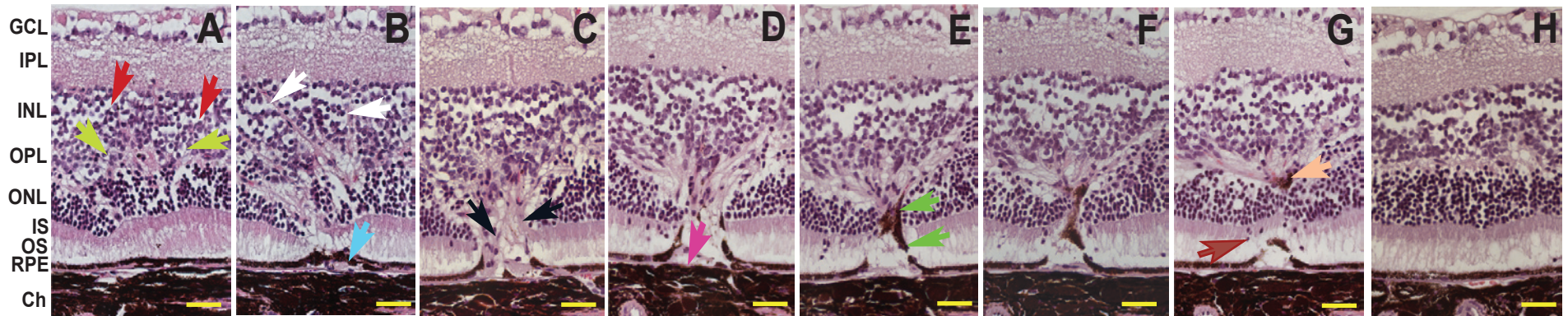


B-G Abnormal Neovascularization in AMD

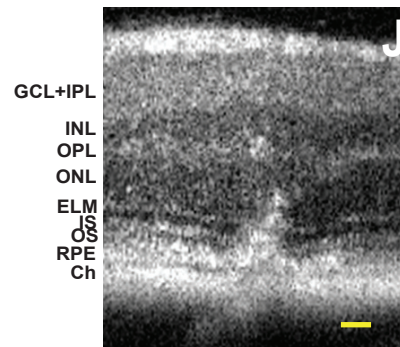
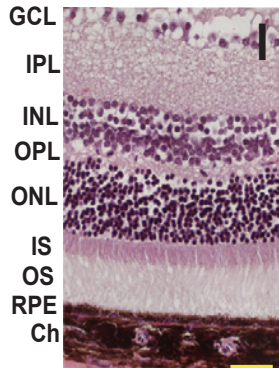


Supplemental Figure 1. Schematic representation of normal retinal vasculature (A) and abnormal neovascularization in AMD (B-G). A, under normal conditions, the mammalian retina has two distinct vascular networks, intraretinal and choroidal. The intraretinal network supplies blood to the inner retina (GCL, IPL, and INL) and is organized into three plexi - superficial, intermediate, and deep - which extend from the GCL to the INL. The choroidal network lies outside the retina and nourishes the outer retina (OPL, ONL, PR, RPE). The OPL is a watershed zone, perfused by diffusion from both the retinal and choroidal networks under normal conditions. In wet AMD, however, there is an abnormal growth of blood vessels (B-G) which proceeds via different scenarios; arising only from the choroid (B,C, and G) or from the retina (D) and retina and choroid (F). Cartoon A is taken with permission from Stahl et al. 2010, IOVS, and modified. Cartoon B is taken with permission from ref(3) and modified.

Cyp27a1^{-/-}



Cyp27a1^{+/+}



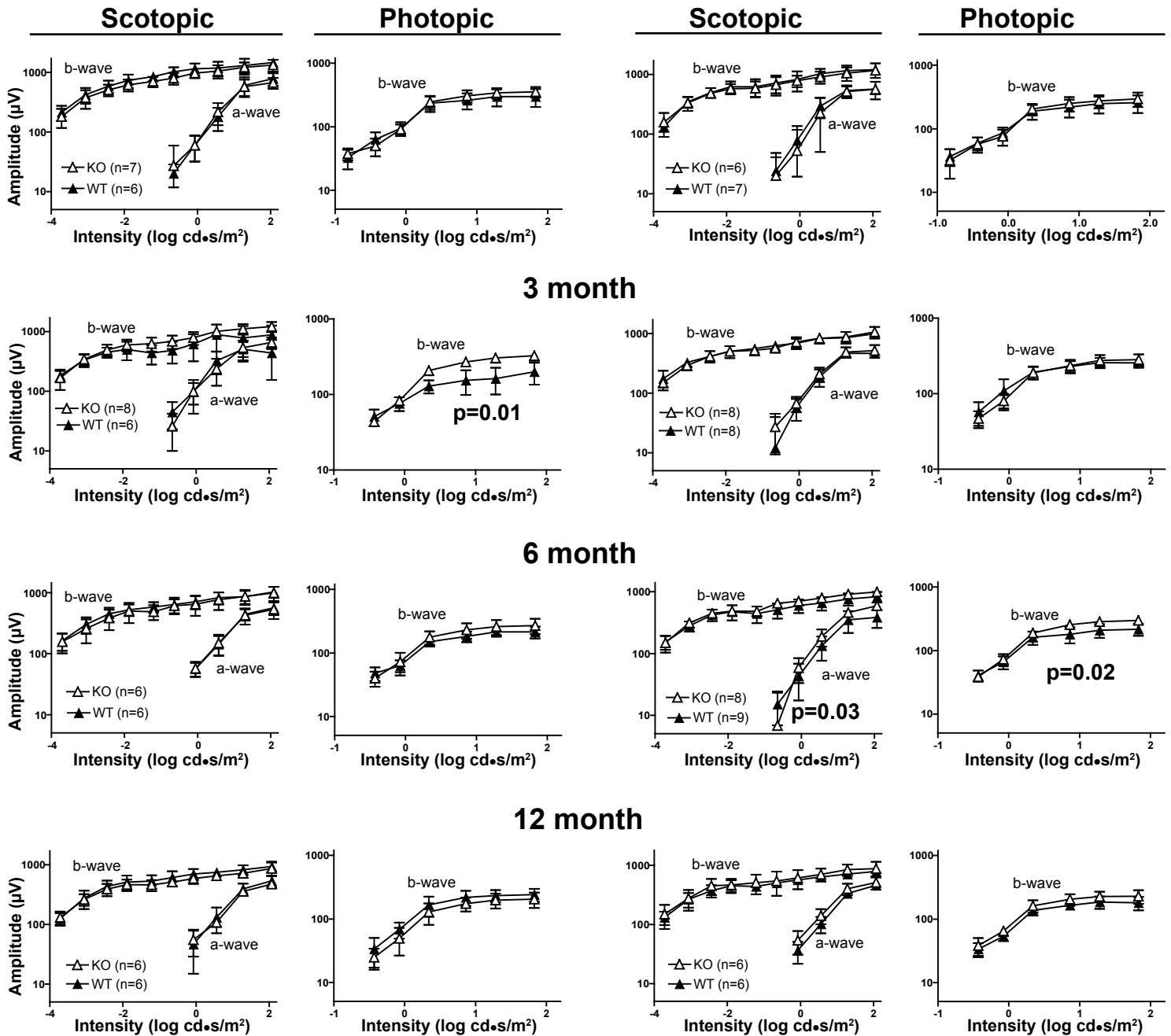
Supplemental Figure 2. Structural changes in *Cyp27a1*^{-/-} mice become more severe with age. Representative H&E staining of serial cross sections through a large area of pathology in a 14 month old *Cyp27a1*^{-/-} mouse (**A-H**) and through a corresponding region in a WT animal (**I**). **J**, SD-OCT cross section from the *Cyp27a1*^{-/-} mouse before sacrifice. This cross section likely corresponds to E or F. Red arrows (**A**) indicate INL edema and vacuolization, light green arrows (**A**) indicate INL nuclei displaced into the disorganized OPL; cyan arrow (**B**) indicates pigmented fibrovascular material above BrM; white arrows (**B**) indicate blood vessels; black arrows (**C**) indicate retinal fibrosis and anomalous vasculature; magenta arrow (**D**) indicates exposure of BrM; green arrows (**E**) indicate RCA; brown arrow (**G**) indicates ONL nuclei displaced into the layers of photoreceptor inner and outer segments; and salmon arrow (**G**) indicates greater RPE tracking into the retinal space than in **Fig. 2H**. Magnification, x400. Scale bars: 30 μ m.

ERG Response in Mice

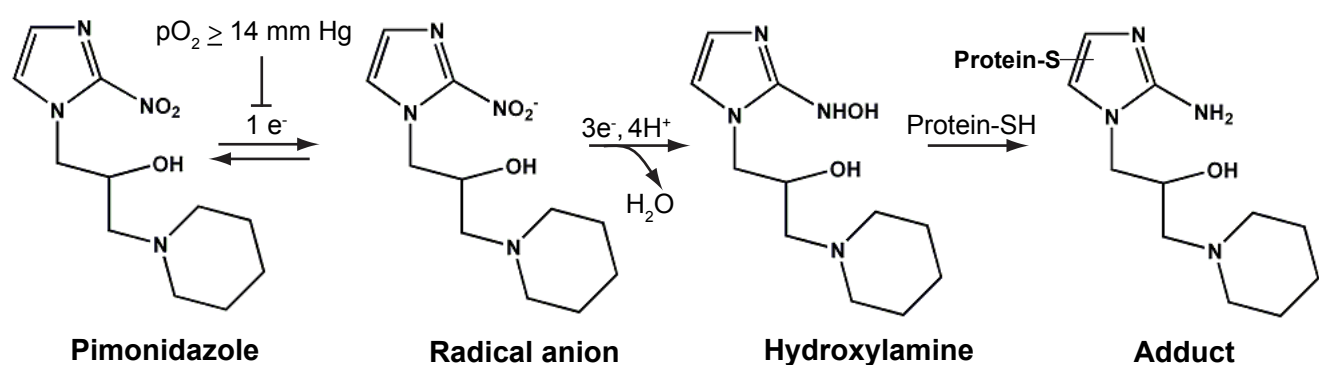
1.5 month

Females

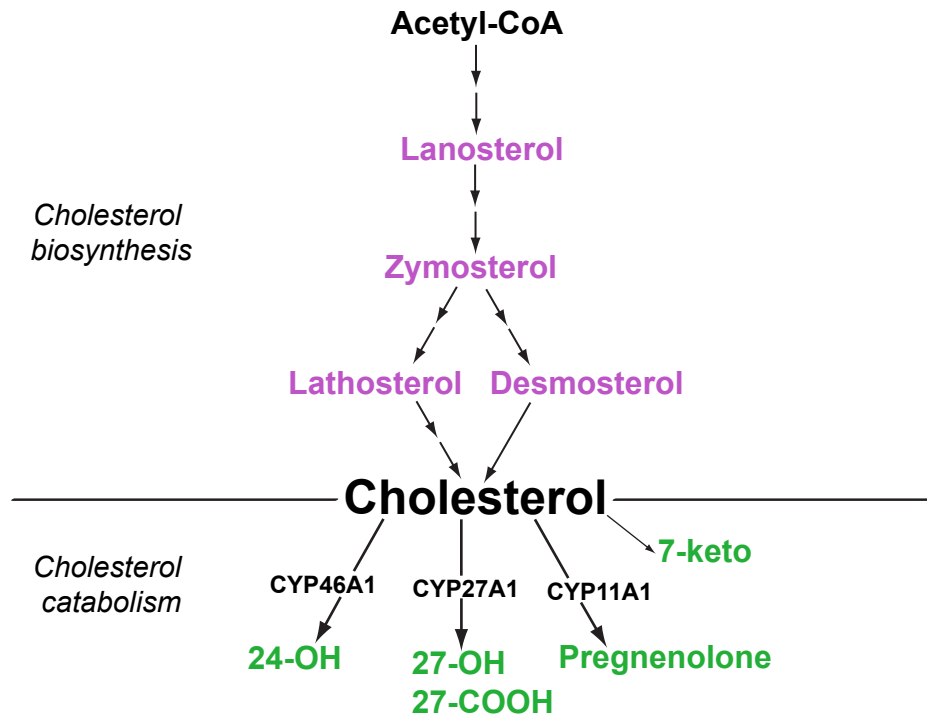
Males



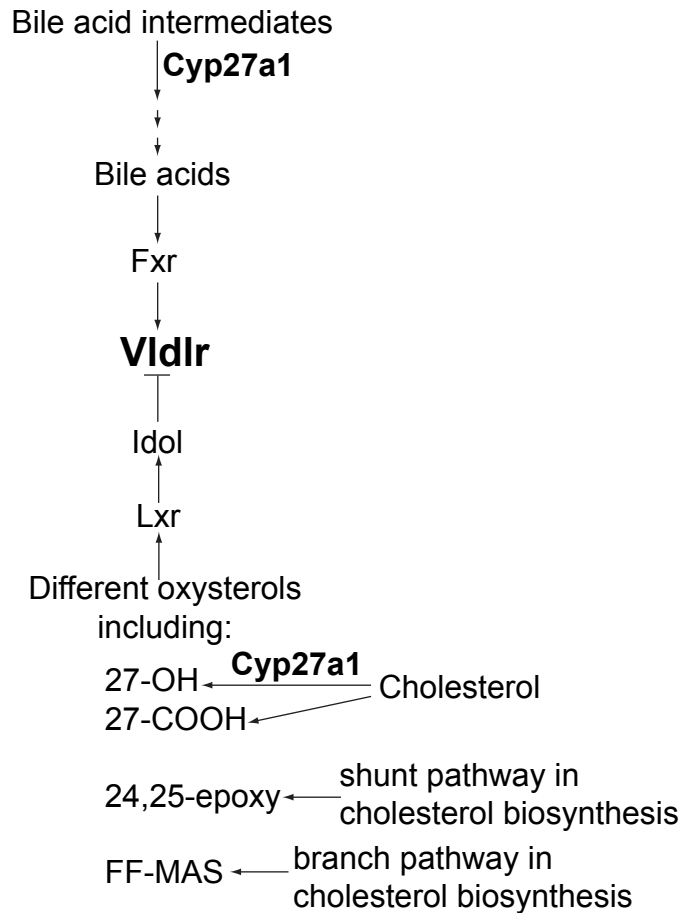
Supplemental Figure 3. ERG response is generally normal in *Cyp27a1*^{-/-} mice. Statistically significant increases in ERG amplitudes are seen only transiently in the photopic b-wave of 3 month old *Cyp27a1*^{-/-} females and in scotopic a- and photopic b-wave amplitudes of 6 month old *Cyp27a1*^{-/-} males. ANOVA with repeated-measures was used for statistical analysis and a p value of ≤ 0.05 was considered significant.



Supplemental Figure 4. Putative mechanism of pimonidazole binding to proteins. At low oxygen tensions (up to 14 mm Hg), pimonidazole sequentially accepts electrons from the cell's transport system to form first a nitro radical anion and then hydroxylamine. The latter reacts with thiol-containing proteins forming stable adducts that can be detected by immunochemical assays. Pimonidazole detects low oxygen tensions and oxygen gradients because its reductive activation in vivo is inhibited by molecular oxygen in a concentration dependent manner with the oxygen tension > 14 mm Hg totally inhibiting reduction of pimonidazole (48).



Supplemental Figure 5. Cholesterol precursors (in magenta) and metabolites (in green) quantified in the present study. In any organ, the steady-state levels of cholesterol are determined by the balance between the input and output pathways. The retina can both synthesize (23, 58-61) and eliminate cholesterol enzymatically. The latter is accomplished via the action of cytochrome P450 enzymes CYP46A1, CYP27A1, and CYP11A1 (27, 28, 64, 65, 70-72). Retinal cholesterol could also be oxidized non-enzymatically to 7-ketocholesterol (75). Accordingly, if one of the pathways contributing to the retinal cholesterol homeostasis is impaired or blocked, like in *Cyp27a1*^{-/-} mice, there may be a compensatory up- or down-regulation of the other pathways manifested in altered levels of cholesterol precursors and/or metabolites. Abbreviations are the same as in Figure 9.



Supplemental Figure 6. Potential mechanisms that could lead to reduced expression of Vldlr in *Cyp27a1*^{-/-} mice. Abbreviations are the same as in Fig. 9. 24,25-epoxy, 24,25-epoxycholesterol; FF-MAS, follicular fluid meiosis-activating sterol.